Role of Magic-Sized Clusters in the Synthesis of CdSe Nanorods

Zhong-Jie Jiang and David F. Kelley*

University of California, Merced, 5200 North Lake Road, Merced, California 95344

ARTICLE

ABSTRACT The dynamics of the CdSe nanorod synthesis reaction have been studied, giving attention to the kinetics of magic-sized clusters (MSCs) that form as intermediates in the overall reaction. The MSCs have a distinct absorption peak, and the kinetics of this peak give insight into the overall reaction mechanism. In these studies, the reaction mixture consists primarily of Cd(phosphonate)$_2$ and trioctyl phosphine selenium in a solution of trioctylphosphine (TOP) and trioctylphosphine oxide (TOPO). We find that the rate at which precursors react to form CdSe monomers and the rates at which monomers react to form nanoparticles can be varied by changing the chemistry of the reaction mixture. Decreasing the TOP concentration decreases the extent to which selenium is bound, both in the precursors and on the particles' surfaces, and thereby increases both the precursor to monomer and monomer to particle reaction rates. Decreasing the phosphonate concentration decreases the extent to which phosphonate binds cadmium in the precursors and on the surface of the nanoparticles, also increasing the rates of both reactions. This is also accomplished by the addition of inorganic acids which protonate the phosphonates. The presence of inorganic acids (impurities) is the primary reason that the overall synthesis reaction is faster in solutions made with technical grade rather than purified TOPO. The TOP and phosphonic acid concentrations are coupled because excess phosphonic acids react with TOP, forming TOPO and less strongly binding species, specifically phosphinic acids, phosphine oxides, and phosphines.

KEYWORDS: CdSe nanorods · synthesis · magic-sized clusters

There are now very effective synthetic methods to produce CdSe nanoparticles having different sizes and shapes.[1−6] In this paper, we will focus on the synthesis of nanorods with controllable sizes and aspect ratios. Most of the recent syntheses of CdSe nanoparticles are variations on a common theme. Cadmium and selenium precursors are reacted in a coordinating solvent at high temperature. The cadmium precursor is a cadmium alkylcarboxylate or alkylphosphonate made by the dehydration of a 1:2 mol ratio mixture of cadmium oxide and an alkyl carboxylic or alkyl phosphonic acid (PA). The syntheses are typically run in excess trioctylphosphine oxide (TOPO),[7] although other solvents can be used.[8] The selenium precursor is elemental selenium dissolved in tributylphosphine (TBP) and/or trioctylphosphine (TOP). The coordinating solvent is the TOPO and TOP from the precursor solutions. In some cases, other Lewis bases, such as alkyl amines, are also added. Nanospheres and nanorods are made in similar ways. The main difference is that the spheres are synthesized from more reactive precursors, typically cadmium carboxylates in a mixture of TOPO and an alkyl amine. CdSe nanorods are synthesized from more strongly bound and therefore less reactive cadmium phosphonates (often octadecylphosphonic acid, ODPA) in a mixture of TOP and TOPO. These methods give controllable rod morphologies while avoiding the use of more toxic and reactive dimethyl cadmium precursors used in earlier syntheses.[9]

The synthesis of CdSe nanoparticles is typically run in an anaerobic, ~300 °C TOPO solution and may be simply written as $Cd(X)_2 + TOPSe \rightarrow CdSe$ (nanoparticles), where X = carboxylate or phosphonate. The $Cd(X)_2$ precursor is typically made from the reaction of the corresponding acid with CdO. In addition to solublizing the cadmium and selenium precursors, the carboxylate or phosphonate and TOP play other roles in the overall reaction. TOPSe is converted to TOPO, and the carboxylate or phosphonate is partially converted to anhydrides. This reaction can be considered to occur in two stages. The first is the reaction of the cadmium and selenium precursors to form CdSe monomers. This is followed by the reaction of the monomers to form nuclei and then nanoparticles. These two steps are not completely separate. It is also possible for the cadmium and selenium precursors to decompose directly on the monomers or on the growing particle surfaces. The first step in the overall synthesis reaction has been carefully studied and is reasonably well understood.[10] In this paper, we focus on how

*Address correspondence to dfkelley@ucmerced.edu.

Received for review January 13, 2010 and accepted February 15, 2010.

Published online March 1, 2010.
10.1021/nn100076f

the chemistry of the reaction mixture affects the second step of the reaction, the reaction of monomers to form nanoparticles. We are particularly interested in the intermediates in this process and how their kinetics are affected by the presence or absence of minor species in the reaction mixture. Consistent with literature reports,[1,11−13] we show below that ODPA and TOP can associate with and control the reactivity of the monomers as well as the different crystal facets of the growing particles.

Cadmium atoms can be bound by carboxylates or phosphonates at different stages of the reaction. The carboxylates or phosphonates are Lewis bases that are the ligands on the cadmium precursors and later bind to the monomers and the surfaces of growing particles. The concentrations of these species therefore determine the reactivities at several different stages of the reaction.[4,14] The difference in the stabilities of cadmium phosphonates compared to cadmium carboxylates initially results in very different precursor reactivities and later to different extents of particle surface binding. In both cases, the selenium precursors are the same (TOPSe) and it is the differences in the ligands associated with the cadmium precursors that result in the different particle morphologies.

The reaction of CdSe monomers to form nanoparticles is, in principle, very simple: monomers nucleate to form very small clusters which subsequently grow into nanoparticles. This simple picture can be complicated by the presence of two different energetically accessible crystal phases, wurtzite and zinc blende. The nanoparticle crystal phase and the reaction kinetics are controlled by thermodynamics of the reaction solution. The crystal phase is critical because different crystal facets of the growing nanoparticle may have different reactivities, and this determines the final morphology of the particles. The solution thermodynamics are determined by the temperature and the chemical composition of the reaction mixture. High temperatures favor the formation of wurtzite particles, while zinc blende particles are grown at lower temperatures.[15] When CdX_2 is reacted with TOPSe in a solution of pure TOP and TOPO, this chemistry is comparatively simple. However, the chemistry of the reaction mixture is greatly complicated by the presence of minor species. These species may bind the reaction precursors, the CdSe monomers, and the surfaces of the nascent CdSe particles. The presence or absence of minor species can therefore result in dramatic changes in the reaction kinetics and the morphologies of the final particles. In some cases, the presence of certain minor species is essential to obtain the desired particles. These minor species may be added deliberately or may be present as impurities in the TOP and TOPO. Technical-grade TOPO is known to contain significant quantities of impurities that can strongly bind cadmium atoms, or alter the binding of other, intentionally added ligands. Their concentrations as impurities vary from one lot of TOPO to another and can lead to synthesis reproducibility problems. The amounts of several of these impurities and their roles in the synthesis of CdSe nanowires have recently been studied.[16,17] These studies identified many of the common impurities and elucidated their roles in controlling the reactivity of the cadmium precursors. The synthesis chemistry of nanorods is quite different and how these species affect the synthesis of CdSe nanorods has not been previously examined.

The overall reaction of cadmium and selenium precursors to form nanoparticles involves several intermediates. As mentioned above, the mechanism and intermediates involved in the initial stage of this reaction, the formation of CdSe monomers, have been studied.[10] The subsequent reaction of monomers to form nanoparticles and the intermediates involved in this reaction are not as well understood. Under some circumstances, "magic-sized clusters" (MSCs) are transiently formed in this reaction. MSCs are very small, well-defined CdSe clusters that exhibit sharp absorption spectra. Intense spectral features characteristic of MSCs are often observed in the synthesis of CdSe nanorods, and their presence in this synthesis has been discussed in terms of the thermodynamics of the reaction. MSCs of CdSe,[4,5,18−25] CdS,[26−29] and CdTe[30,31] have been the subject of numerous studies. It has been suggested that these species correspond to local thermodynamic minima in the progression from precursors to final nanorods and are formed only at the high monomer chemical potentials needed to form the rod morphology.[4,5,18] Despite having been observed in the CdSe nanorod synthesis and studied in synthesis reactions, their role as intermediates in the overall production of CdSe nanorods has not been elucidated.

Scope of This Paper. In this paper, we present a systematic study of the overall reaction mechanism for CdSe nanorods. The study examines the concentration dependence of both major and some of the minor chemical species in controlling the rates at which cadmium and selenium precursors react to form monomers and the monomers form and grow nanoparticles. Much of the focus of this paper is on the role of MSCs as intermediates in the overall reaction. Since the MSC and nanoparticle concentrations are easy to follow spectroscopically, these kinetics are used to probe the reaction mechanism. Throughout the kinetic analysis, we use the same thermodynamic considerations that have been previously used to analyze the CdSe synthesis reactions. This treatment is combined with the same ideas used to understand the effects of impurities in the synthesis of CdSe nanowires.[16,17] Experimental results are presented to elucidate the roles of major species and minor species at concentrations relevant to commercial technical-grade TOP and TOPO. Specifically, we show that the Cd/phosphonate and Se/TOP ratios have significant effects on the overall reactivity. We also examine the effect of chain length in the alkyl phosphonates

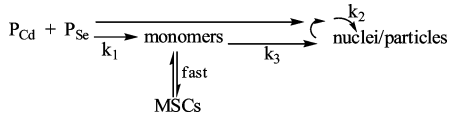

Scheme 1.

on the precursor, monomer, and particle surface reactivities. Lastly, we also show that the presence of inorganic acids at concentrations typically seen in technical-grade TOPO results in protonation of the cadmium precursor, greatly increasing its reactivity.

RESULTS AND DISCUSSION

In what follows, we propose a mechanism for the overall synthesis reaction and the role of MSCs in this reaction. This mechanism is discussed in terms of the thermodynamics of the monomers, MSCs, and final nanoparticles. We show that many of the literature results can be understood in terms of the proposed mechanism. This is followed by presentation of kinetic results from several different syntheses performed with different reaction conditions. These kinetics are modeled in terms of the proposed mechanism, and the results are discussed in terms of known aspects of CdSe nanoparticle syntheses.

Proposed Mechanism and the Thermodynamics of the CdSe Nanorod Synthesis Reaction. The reaction of cadmium phosphonate in TOPO (the cadmium precursor) and TOPSe in TOP/TBP (the selenium precursor) to produce CdSe nanorods proceeds in several distinct stages. Initially, the precursors react to form CdSe monomers. The rate of monomer formation depends on the precursor reactivities and determines the monomer concentration early in the reaction. As the reaction proceeds, MSCs may be formed. Under conditions in which nanorods are synthesized, the most persistent MSC has an intense and very sharp absorption peak at 350 nm. These MSCs are believed to have a well-defined morphology, corresponding to a Cd_{17} tetrahedral cluster of zinc blende CdSe.[4,5,20,21] The zinc blende structure of these MSCs is important because CdSe nanorods grown under these conditions have exclusively wurtzite structure. (The unique axis of the wurtzite structure determines the long axis of the nanorod.) Thus, the MSCs have the wrong structure to be able to easily go on to form nanorods. The MSCs are therefore a "dead end" in the reaction mechanism, rather than an intermediate between monomers and nanoparticles. We propose the overall reaction mechanism and intermediates depicted in Scheme 1.

In this mechanism, the cadmium and selenium precursors (P_{Cd} and P_{Se}, respectively) react to form CdSe monomers with a rate constant of k_1. The monomers react to form nanoparticle nuclei and react with existing nuclei and particles to grow the particles with a total phenomenological first-order rate constant of k_3. In addition, the precursors can react directly on the particle surfaces, providing a separate path for particle growth. This rate depends on the total particle surface area which is assumed to scale like the number of monomer units in the particles to the 2/3 power and is described by a phenomenological rate constant of k_2. A central feature of this proposed mechanism is that the MSCs are in equilibrium with the monomers. The monomer concentration is therefore limited to the saturation value, M_0, at which the monomers condense to form MSCs. The formation and dissolution of the MSCs are assumed to occur rapidly, maintaining this equilibrium. The result of this equilibrium is that, when MSCs are present, monomer formation or depletion reactions simply change the MSC concentration. Thus, the fast equilibrium with the MSCs provides a reservoir that holds the monomer concentration constant at M_0. A set of kinetic equations can be derived from Scheme 1 and are as follows.

$$d(P_{Cd})/dt = d(P_{Se})/dt = -k_1(P_{Cd})(P_{Se}) - k_2(P_{Cd})(P_{Se})(NP)^{2/3} \quad (1)$$

$$\begin{aligned} d(M)/dt &= k_1(P_{Cd})(P_{Se}) - k_3(M) \quad M < M_0, MSC = 0 \\ d(M)/dt &= 0 \qquad\qquad\qquad\quad MSC > 0 \end{aligned} \quad (2)$$

$$\begin{aligned} d(MSC)/dt &= k_1(P_{Cd})(P_{Se}) - k_3(M) \quad M \geq M_0, MSC > 0 \\ d(MSC)/dt &= 0 \qquad\qquad\qquad\quad M < M_0 \end{aligned} \quad (3)$$

$$d(NP)/dt = k_3(M) + k_2(P_{Cd})(P_{Se})(NP)^{2/3} \quad (4)$$

These equations can be numerically integrated to give time-dependent MSC and nanoparticle concentrations, which may be compared to experimental values. The model has several adjustable parameters: M_0, k_1, k_2, k_3. Fitting the experimentally determined time-dependent MSC and nanoparticle absorbances also requires that the ratio of MSC to nanoparticle extinction coefficients be taken as an adjustable parameter. However, once the values of M_0 and the extinction coefficient ratio are determined, they do not vary as the solution chemistry is changed.

This proposed mechanism is consistent with the thermodynamic considerations discussed by Peng *et al.*[1,4,5,18,19] Specifically, the chemical potentials of each of the reactive species (monomers, MSCs, nuclei, and size- and aspect-ratio-dependent nanorods) determine the course of the reaction. The monomer chemical potential increases with increasing concentration. The chemical potentials of the nanoparticles are size- and shape-dependent, generally increasing with the surface to volume ratio. Thus, the chemical potential of particles generally increases with decreasing size, and for a given volume, nanorods have a higher chemical potential than nanospheres. However, a plot of chemical potential *versus* size has local minima corresponding to different magic-sized clusters. The MSCs observed in nanorod syntheses are believed to correspond to a Cd_{17} species. There are surely several sizes of wurtzite MSCs, and the wurtzite clusters having the highest chemical potential may be thought of as the nuclei from which

the nanorods grow. However, under the present conditions, these species are unstable with respect to growth into nanoparticles. These magic-sized clusters are not observed and will not be considered further. In contrast, growth of the zinc blende MSCs giving rise to the 350 nm peak would lead to the less stable zinc blende particles and therefore does not occur. Because these MSCs are all the same size, they have a well-defined chemical potential. Associated with the MSCs is a well-defined monomer saturation concentration, M_0.

Several monomer concentration regimes can be identified and defined in terms of the monomer chemical potential (μ_m) compared to the chemical potentials of the MSCs (μ_{msc}), wurtzite nuclei (μ_n), nanorods (μ_{nr}), and nanospheres (μ_{ns}). Nanorods can be formed under conditions in which the monomer concentrations are too low to form MSCs (see below). This observation establishes that $\mu_{msc} > \mu_n > \mu_{nr} > \mu_{ns}$. In order of decreasing monomer concentration, the different regimes for μ_m are as follows.

(1) MSC equilibrium, $\mu_m = \mu_{msc}$. Monomers react to form nuclei ($\mu_m > \mu_n$) and are in equilibrium with MSCs.

(2) MSC dissolution/particle nucleation and growth, $\mu_{msc} > \mu_m > \mu_n > \mu_{nr}, \mu_{ns}$. MSCs are not yet formed or have dissolved to form monomers, but the monomer concentration is high enough for nucleation to occur. The monomers react with nuclei and/or small particles causing particle growth.

(3) Particle growth, $\mu_{msc} > \mu_n > \mu_m > \mu_{nr}, \mu_{ns}$. There are no MSCs, and nucleation does not occur, but particle growth continues. A higher chemical potential is needed to cause nanorod compared to nanosphere growth.

(4) Rod to sphere ripening, $\mu_{nr} > \mu_m > \mu_{ns}$. Rods ripen to spheres, lowering the aspect ratio but leaving the particle volume unchanged.

(5) Ostwald ripening, $\mu_{ns} > \mu_m$. Particles undergo Ostwald ripening, broadening the size distribution.

Upon precursor injection, the monomer concentration is fed by precursor reaction and rises rapidly. The monomer concentration soon exceeds that necessary for particle nucleation, and particle formation starts. This concentration may continue to rise, and upon reaching M_0 (corresponding to $\mu_m = \mu_{msc}$), MSCs and their characteristic 350 nm peak appear. When reaction of the monomers causes this concentration to drop below M_0, the MSCs dissolve and the 350 nm peak disappears. In Scheme 1, MSCs can act as a reservoir, holding the monomer concentration at M_0. Because the concentration of MSCs is related to the production and depletion of monomers, the formation and disappearance kinetics of the MSC absorption peak at 350 nm are diagnostic of the time-dependent monomer concentrations. Thus, the intensity and duration of the MSC peak along with the growth of the exciton absorption provide the measure of k_1, k_2, k_3, and M_0. In the latter stages of the reaction, the MSCs have dissolved and precursors are depleted, so the monomer concentration falls.

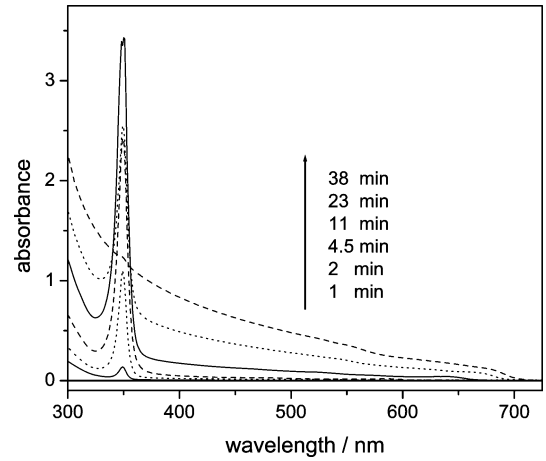

Figure 1. Absorption spectra of a CdSe synthesis in which the Cd/ODPA/Se/TBP+TOP mol ratio is 1:2.0:0.5:3.0. In this synthesis, the TOPSe/TOP/TBP solution is injected into a solution of Cd(ODPA)$_2$ in purified TOPO. The reaction is run at 300 °C. Spectra are taken 1 (solid), 2 (dot), 4.5 (dash), 11 (solid), 23 (dot), and 38 (dash) min after injection.

If the monomer concentration is too low, then $\mu_{nr} > \mu_m > \mu_{sp}$, and only spherical growth is possible, causing the rods to ripen into spheres. The growth of high quality, high aspect ratio nanorods therefore requires that the reaction be quenched before the monomer concentration drops that far. This regime has been carefully studied.[18] The present study examines the initial stages of the reaction during which the monomer concentration is relatively high, MSCs are formed and redissolve, and particle growth occurs.

Previous studies have shown that the cadmium precursor reactivity can be controlled in several ways, most of which affect all of the rates in Scheme 1. The stability of the precursor depends on the base to which the cadmium is bonded. Cadmium forms weaker bonds to carboxylates than to phosphonates, making the former a more reactive precursor. Furthermore, the reactivity of Cd(phosphonate)$_{2-x}$(carboxylate)$_x$ increases with the value of x.[17] This changes the precursor reaction rate constants (k_1 and k_2 in Scheme 1). However, the precursor and monomer reaction rates (k_3 in Scheme 1) are strongly coupled. This is because, when the precursors react to form CdSe monomers, the carboxylate or phosphonate bases or their anhydrides are available to subsequently bind the monomers and/or the particles' surfaces.[10−12]

"Standard Nanorod Synthesis" with Pure Reagents. The simplest CdSe nanorod synthesis involves the cadmium precursor made from CdO and ODPA at a 1:2 mol ratio in purified TOPO, and the selenium precursor is made from elemental selenium dissolved in purified TBP/TOP.[4,6] The selenium precursor is injected into the cadmium precursor at 320 °C, and the reaction is run at 300 °C. Spectra for this reaction at various times following injection are shown in Figure 1. At 2 min into the reaction, a weak, but well-defined, exciton peak appears at 523 nm. As the reaction proceeds, this peak gains in intensity and shifts to the red, characteristic of particle

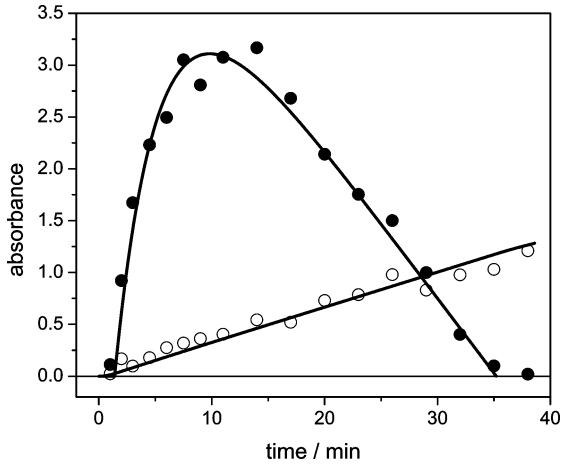

Figure 2. Kinetics of the MSC peak (solid circles) and the 350 nm baseline (open circles). These data are taken from Figure 1. Also shown are curves calculated from eqs 1−4 with M_0 = 8.1 mM and the rate constants given in Table 1.

growth. The reaction is stopped after 38 min. At this point, the absorption onset is at 705 nm, indicating large particles exhibiting minimal quantum confinement. TEM images are qualitatively similar to those previously reported[32] and indicate that the final particles produced by this reaction are nonbranched nanorods. This is important because growth from zinc blende MSCs would likely result in branched nanoparticles. Consistent with the red-shifted spectrum, these nanorods are quite large, having diameter and length dimensions of 6.05 ± 0.88 and 39 ± 4.9 nm, respectively. The spectra of the reaction mixture show a very prominent absorption peak at 350 nm, which is assigned to MSCs. The MSC peak appears almost immediately after selenium precursor injection, has its maximum intensity at about 14 min, and disappears after about 35 min. This reaction mixture is the least reactive of any studied here, resulting in a very high concentration of MSCs, which persist for a relatively long time. The time dependence of the MSC peak (subtracting off the underlying baseline) and the 350 nm baseline absorption under the MSC peak are plotted in Figure 2. The time dependence of the 350 nm baseline absorbance is also plotted in Figure 2. All CdSe nanoparticles have a significant absorption at 350 nm, and this baseline absorbance is roughly indicative of the total concentration of CdSe in the form of nanoparticles.

Perhaps the most striking thing about these kinetics is the sudden loss of the MSC absorption at about 35 min. Specifically, from the kinetics shown in Figure 2, it is obvious that $d(MSC)/dt \neq 0$ as MSC $\rightarrow$ 0 at 35 min. This is not unique to this sample but is consistently observed in all samples for which the 350 nm peak is present. From this qualitative observation alone, one can conclude that the primary process controlling the rate at which MSCs are lost is not the reaction of the MSCs to form nanoparticles. If reaction with monomers was the rate-determining step in the disappearance of MSCs, then the rate would slow as either the monomer or MSC concentration decreased, and one would find that $d(MSC)/dt = 0$ at MSC $\rightarrow$ 0. This observation is the basis for the central idea in Scheme 1: that the MSCs are in equilibrium with the monomers and that the forward and reverse rates that maintain this equilibrium are faster than the rates that form and deplete the monomers. Curves calculated by numerically integrating eqs 1−4 are also shown in Figure 2. Good agreement with the experimental results is obtained, with the calculated curves reproducing the essential features of the observed kinetics. The calculated curves in Figure 2 correspond to the following values of these parameters: M_0 = 8.1 mM, k_1 = 0.25 L mol^{-1} min^{-1}, k_2 = 0.15 (L/mol)$^{5/3}$ min^{-1}, and k_3 = 0.072 min^{-1}. The M_0 value indicates that the highest possible monomer concentration is 8.1 mM, corresponding to a monomer-saturated solution at 300 °C. Figures 1 and 2 show that the baseline absorbance increases approximately linearly with time over the first 35 min of the reaction, that is, when MSCs are present. This is easily understood in terms of the mechanism of particle nucleation and growth. Growth occurs primarily from monomer deposition on the surfaces of existing particles. When MSCs are present, the monomer concentration is constant at M_0, resulting in a constant growth rate.

It is also of interest to compare the above value of k_1 with kinetic results by Liu *et al.*[10] By measuring the disappearance of TOPSe by ^{31}P NMR, a first-order rate constant of $k = 1.7 \times 10^{-3}$ s^{-1} was obtained. This result was obtained with an initial cadmium concentra-

TABLE 1. Maximum Absorbances, Disappearance Times of the MSC Peak, and Rate Constants (*Scheme 1*) for Differing Selenium and TOP Concentrations

	standard synthesis	decreased TOP	increased selenium	constant ratio	decreased selenium
Se concn (mmol)	0.8[a]	0.8[b]	1.07	0.6	0.6[c]
TOP concn (mmol)	3.0[a]	2.25[b]	3.0	2.25	3.0[c]
MSC maximum absorbance	3.1	0.8	0.50	2.0	0.40
MSC disappearance time (min)	35	8.0	4.5	21	8.0
k_1 (L mol^{-1} min^{-1})	0.25	0.48	*d*	0.35	0.35
k_2 (L/mol)$^{5/3}$ min^{-1})	0.15	0.82	*d*	0.15	1.75
k_3 (min^{-1})	0.072	0.27	*d*	0.075	0.22

[a]Results are shown in Figures 1 and 2. [b]Results from Figure 3a. [c]Results from Figure 3b. [d]MSC peak is too short-lived to allow extraction of rate constants.

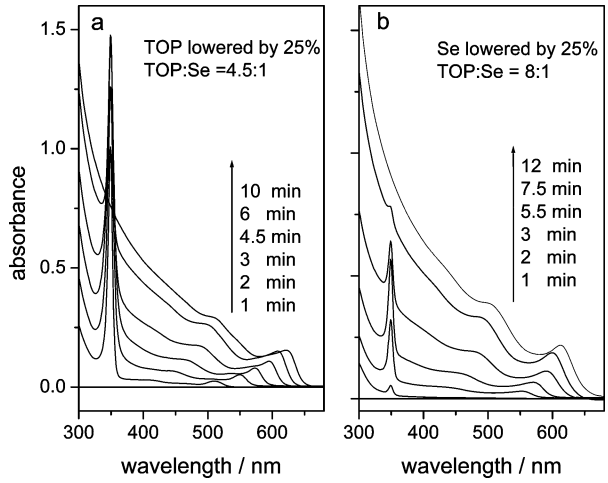

Figure 3. Absorption spectra of a CdSe synthesis in which the Cd/ODPA/Se/TBP+TOP mol ratios are (a) 1:2.0:0.5:2.25 and (b) 1:2.0:0.375:3.0. In this synthesis, the TOPSe/TOP/TBP solution is injected into a solution of $Cd(ODPA)_2$ in purified TOPO. The reaction is run at 300 °C, and the spectra are taken at the times indicated in each panel.

tion of 0.27 M and without precursor aging. The calculated curves in Figure 2 correspond to a second-order rate constant of $k_1 = 0.25$ L mol^{-1} s^{-1}. The initial concentrations are $P_{Cd} = 0.22$ M and $P_{Se} = 0.11$ M. In the absence of reaction with nanoparticles, this corresponds to a pseudo-first-order rate of 0.059 min^{-1} $= 1 \times 10^{-3}$ s^{-1}. We note that the studies by Liu *et al.* use an initial cadmium precursor concentration that is 25% higher than in present studies. If the same cadmium precursor concentration had been used in the present studies, Scheme 1 predicts a 25% higher pseudo-first-order rate constant, 1.25×10^{-3} s^{-1}. We conclude that the precursor reaction rate constant obtained through this modeling is in good agreement (within 50%) with that obtained using a completely different method of determining the rates. There are two factors which may contribute to the slightly larger rate constant measured by Liu *et al*. First, in the syntheses reported here, the cadmium precursor is aged, which reduces its reactivity.[4] Second, there are differences in the chemistry of the reaction mixture, specifically, Liu *et al.* use a lower TOP to selenium ratio than that used here. The effects of varying the solution chemistry are examined next.

Effects of Varying the Selenium, TOP, and ODPA Concentrations. Changing the concentrations of any of the components in the reaction mixture can have dramatic effects on the reaction kinetics and the dimensions of the final particles. The simplest way to view the kinetic results is in terms of the intensity and duration of the MSC peak. Although it is always, in principle, possible to fit the MSC absorption kinetics and extract rate constants, it is often difficult to obtain a unique set of values. This is because it is difficult to discriminate between particle formation and growth from precursors and from monomers, the reaction pathways associated with rate constants k_2 and k_3, respectively. This is particularly true when the reaction is fast and the MSC peak is present for only a brief period of time. However, fitting the kinetics of the less reactive solutions indicates that the k_2 pathway is typically minor, but not insignificant. As such, the calculated curves are relatively insensitive to the exact value of k_2. The maximum MSC intensity is controlled by the ratio of overall monomer formation and loss rates. A very intense and long-lived MSC peak indicates relatively rapid monomer formation and slow monomer loss. These considerations indicate that the maximum intensity and duration of the MSC peaks give qualitative insights into the relative monomer formation and loss rates in Scheme 1. The maximum intensities and disappearance times of the MSC peaks and fitted values for the rate constants in eqs 1−4 under different reaction conditions are collected in Table 1.

The effects of changing the selenium and TOP concentrations are strongly coupled, and the TOP to selenium ratio has a large effect on the solution reactivity, as shown in Figures 3 and 4. Figure 3 shows the effects of varying the TOP to selenium ratio. If the TOP concentration is lowered by 25% and selenium concentration is held constant, the progress of the reaction changes dramatically. Figure 3a shows the spectra of the reaction run with these concentrations. Comparison with Figure 1 shows that the reaction proceeds much more rapidly and that the MSC peak is both less intense and shorter lived. Comparison of the standard synthesis and decreased TOP columns of Table 1 indicates that the maximum MSC absorbance is reduced from 3.1 to 0.8, and the disappearance time is reduced from 35 to 8 min. The kinetics of the reaction with decreased TOP are shown in Figure 4. The rate constants used to calculate the kinetic curves in Figures 2 and 4 are also given

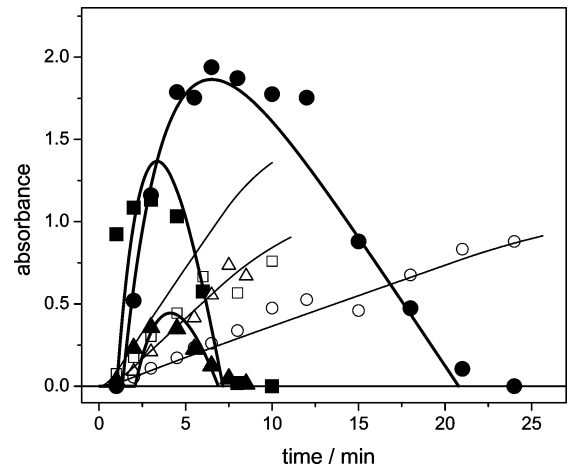

Figure 4. Kinetics of the MSC peak (solid symbols) and the 350 nm baseline (open symbols) of CdSe syntheses in which the Cd/ODPA/Se/TBP+TOP mol ratios are 1:2.0:0.375:2.25 (constant ratio, circles), 1:2.0:0.375:3.0 (decreased Se, squares), and 1:2.0:0.5:2.25 (decreased TOP, triangles). Curves calculated from eqs 1−4 and Table 1 for MSC (thick lines) and the particle (thin lines) absorption intensities are also shown. M_0 is taken to be 8.1 mM in all cases.

in Table 1. The same effect is observed if the TOP concentration is held constant and the selenium concentration is raised, as indicated in the increased selenium column of Table 1; the reaction proceeds more much rapidly with the MSC peak becoming less intense and shorter lived. These results indicate that the precursor to monomer reaction, and to a greater extent the monomer to nanoparticle reaction, becomes faster as the TOP to selenium ratio is reduced. This suggests that TOP molecules bind and stabilize the TOPSe precursor and, to a larger extent, the CdSe monomers and/or the selenium atoms on the growing nanorod surface. A decreased TOP to selenium ratio increases both selenium precursor and particle reactivities. Consistent with this explanation, if both the selenium and the TOP concentrations are reduced by 25%, there is only a modest decrease in the maximum MSC intensity and duration; compare the standard synthesis and constant ratio columns of Table 1. The constant ratio rate constants are less than 50% larger than those obtained for the standard synthesis. However, Figure 3b and the decreased selenium column of Table 1 show that reducing the selenium concentration at a constant TOP concentration also increases the reactivities. We suggest that this is due to the reaction of TOP with ODPA (discussed below), and this result can be understood only after examining the role of ODPA in determining the reactivities.

The mol ratio of cadmium to the alkyl phosphonic acid (ODPA in this case) also has a large effect on the solution reactivity. The usual cadmium to ODPA ratio of 1:2 gives a minimum in the reactivity; increasing or decreasing the amount of ODPA in the cadmium precursor increases the reactivity of the precursors. If 25% of the ODPA is put in the selenium precursor (the Cd/ODPA ratio in the cadmium precursor is 1:1.5), the reaction proceeds very rapidly and there is no MSC peak at all. The rapid appearance of particles means that the reaction rate of the precursors to form monomers and the reaction rate of the monomers to grow particles are both increased. The former is easy to understand. In a cadmium precursor with less ODPA than the usual 1:2 stoichiometry, some of the cadmium atoms are bound to a single phosphonic acid and are therefore not as stable as those bound to two phosphonic acids. Peng *et al.*[4] have noted that aging of the Cd(phosphonate)$_2$ precursors decreases their reactivities, presumably because, in the aged precursor, the cadmium is bound to two oxygens on both phosphonates. The precursors with less ODPA than a 1:2 stoichiometry are similar to freshly prepared Cd(phosphonate)$_2$ precursors in that they also have cadmiums that are not fully bound to phosphonic acids. The greater cadmium precursor reactivity seen here is therefore consistent with the observation that the aged cadmium precursors are more stable and less reactive than those that are not. The latter observation, the fast overall reaction and the lack of an MSC peak, indicates an increase in the monomer to particle reaction rate. This observation is very general, and more rapid reaction occurs whenever there is ODPA in the selenium precursor or excess ODPA in the cadmium precursor. Figure 5 shows spectra obtained from syntheses with a Cd/ODPA ratio of 1:2.5, rather than the usual 1:2 ratio. The effects of having the excess ODPA in the cadmium compared to the selenium precursor are shown. In both cases, a significant increase in reactivity is observed (compare Figure 5 with Figure 1). The MSC peak is of much lower intensity and disappears after 2 or 3 min. In this case, the MSC peak disappears too quickly to extract rate constants, but the comparison of Figures 1 and 5 in the context of Scheme 1 shows that both monomer formation and loss rates are very high. The reason for the rapid monomer to particle reaction is elucidated by the comparison of the spectra obtained with the excess ODPA in the cadmium *versus* selenium precursors. When the excess ODPA is added to the selenium precursor, the exciton peak grows more rapidly and shifts further red and the MSC peak disappears more rapidly, compared to when the ODPA is in the cadmium precursor. These results, taken together, indicate that the presence of ODPA in excess of 2.0 times the amount of cadmium increases the reactivity of the selenium precursor as well as that of the monomers and/or particle surfaces. There are several mechanisms by which this increased reactivity can occur. A reaction mechanism for the production of CdSe monomers has recently been proposed in which the TOPSe is activated by nucleophilic attack of the phosphorus by a phosphonic acid. An increase in the phosphonic acid concentration could facilitate this step in the mechanism and thereby increase the reactivity.[10] However, in this case, the reaction would be faster independent of whether the phosphonic acid came in with the cadmium or selenium precursor. This idea also fails to explain why the subsequent monomer to particle rate increases more than the precursor reaction rate. While this mechanism may be occurring, the observation that there is a significant difference in reactivities

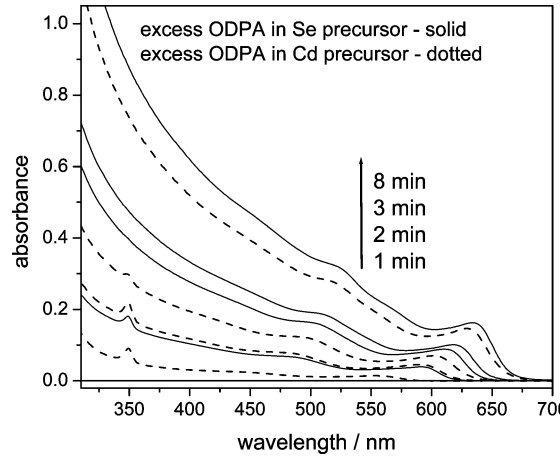

Figure 5. Comparison of syntheses having cadmium to ODPA mol ratios of 1:2.5. The dotted curve has all of the ODPA in the cadmium precursor. The solid curves have 20% of the ODPA in the selenium precursor.

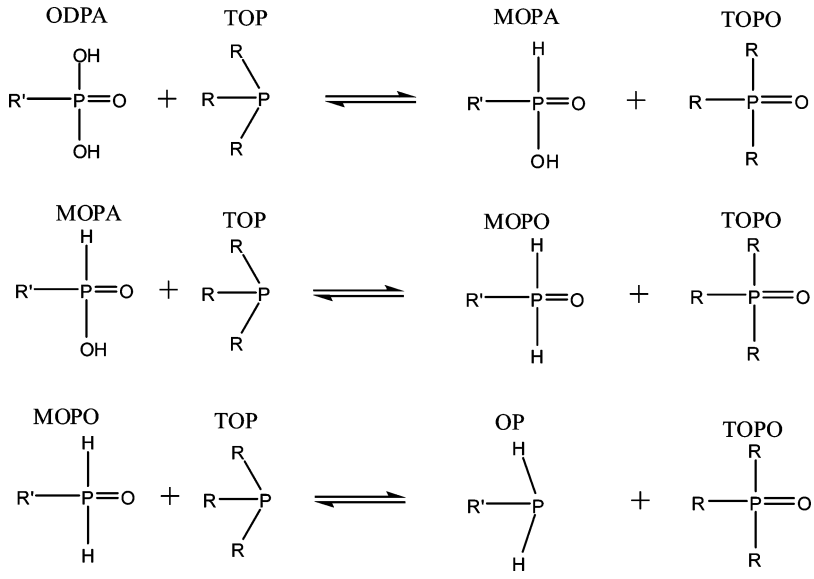

Scheme 2.

depending on which precursor it comes in with suggests that this is not the only mechanism of increased reactivity.

We suggest another reason for the increased reactivity associated with increasing the TOP or the ODPA concentrations: alkyl phosphonic acids react with TOP to form TOPO. The basic idea is that excess (unbound) TOP reacts with ODPA and *vice versa*. The nature of the TOP/ODPA reaction is elucidated by GCMS and ^{31}P NMR spectra of TOP and TOP/octyl phosphonic acid (OPA) mixtures. In deuterochloroform, the TOP, OPA, and TOPO peaks are observed at −31.1, 36.5, and 48.2 ppm, respectively, consistent with literature values.[33] Addition of a small amount of OPA to TOP results in almost no OPA peak. Instead, a TOPO peak appears. GCMS results show the same chemistry. These observations may be understood in terms of the set of oxidative equilibria given in Scheme 2.

The net reaction is ODPA + 3 TOP → octylphosphine (OP) + 3 TOPO. Monooctyloctyl phosphinic acid (MOPA) and monooctyl phosphine oxide (MOPO) are intermediates, in equilibrium with the ODPA, TOP, and TOPO. TOP is a better Lewis base than OP, so the equilibrium of the net reaction favors TOPO. We conclude that, when ODPA is added to the selenium precursor, a significant amount of the TOP is converted to MOPA, MOPO, and TOPO. The same thing happens following injection, albeit to a lesser extent, when excess ODPA is added to the cadmium precursor. Unlike TOP, TOPO and the intermediate species (MOPA and MOPO) do not form complexes with selenium atoms and, therefore, do not stabilize the TOPSe precursor, the selenium in the monomers, or selenium sites on the nanoparticles. Thus, replacing some of the TOP with these species increases the solution reactivity. Similarly, excess TOP reduces the amount of ODPA present and, therefore, increases the cadmium reactivities. This mechanism and the one proposed by Liu *et al.*[10] are probably both involved in explaining these reactivities.

Role of Alkyl Chain Length: Octyl Phosphonic Acid *versus* Octadecyl Phosphonic Acid. The particle aspect ratio can be controlled by changing the chain length of the alkyl phosphonic acid used in the cadmium precursor. For example, syntheses using ODPA and OPA give particles with aspect ratios of 2.5 and 10, respectively.[6] There are two reasons why the alkyl chain length could affect the particle aspect ratio. First, the alkyl chain length affects the extent to which the particle radial surfaces are bound and hence the reactivity of these surfaces. Shorter alkyl chains have less steric interference and can therefore more completely bind the surface cadmium atoms. Strongly bound radial surfaces result in lower radial growth rates and hence larger particle aspect ratios. This is known to occur on growing CdSe nanorods[6] but has not been shown to be the factor that controls the particle morphology. Second, the alkyl chain length affects the precursor reactivity. This is relevant because the precursor reactivity controls the monomer chemical potential, and as discussed above, high monomer chemical potentials are needed to promote the growth of large aspect ratio nanorods. Upon the basis of comparison with alkyl carboxylic acids,[34] the longer chain phosphonic acids are believed (correctly) to form more stable precursors than shorter chain phosphonic acids. However, precursor reactivity arguments cannot explain all of the reported observations. Wang *et al.*[6] have shown that the longer chain, *less reactive* ODPA precursors give *lower aspect ratio* particles than are obtained with the more reactive, shorter chain OPA precursors. However, Peng *et al.*[4] observed that aged precursors are *less reactive* and give rise to *higher aspect ratio* nanorods. The comparison of aged *versus* non-aged precursors is a good one because the chemistry of the reaction mixture is the same; all that is changed is the precursor reactivity. Taken together, these observations suggest that both of the above considerations must play some role in controlling the particle morphology. Shorter alkyl chains result in higher monomer concentrations and more effectively block particle growth on the radial, but not axial, surfaces, thereby producing higher aspect ratio particles.

To further elucidate the roles of these two mechanisms, we have done syntheses in which the cadmium precursor is either cadmium and ODPA in a 1:2 ratio or cadmium, ODPA, and OPA in a 1:1.5:0.5 ratio. In both cases, 0.8 mmol of ODPA is added to the selenium precursor to increase the overall reactivity of the solution and give smaller and more monodisperse nanorods.

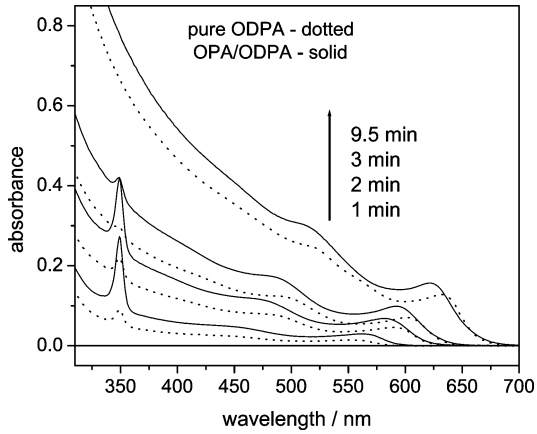

Figure 6. Comparison of absorption spectra from the syntheses having Cd/ODPA of 1:2.5 (20% in the selenium precursor) and Cd/ODPA/OPA mol ratio of 1:2.0:0.5 (25% of the ODPA in the selenium precursor). The times at which the spectra were taken are indicated in the figure.

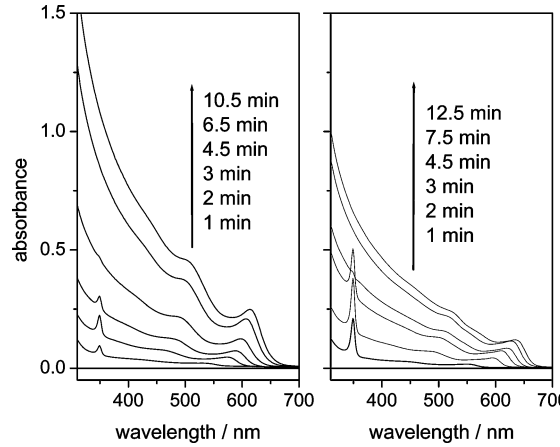

Figure 7. Absorption spectra of a CdSe synthesis in which TOPSe/TBP/TOP is injected into a solution of $Cd(ODPA)_2$ in TOPO. The reactions are analogous to that in Figure 1, except the cadmium precursor was made with (left) technical-grade TOPO and (right) TOPO having 1 mol % of H_3PO_4. The times at which the spectra were taken are indicated in the figures.

Spectra taken at several times during these syntheses are shown in Figure 6. Initially (1 min), the pure ODPA synthesis has a lower concentration of MSCs and a less intense exciton peak. The exciton peak is also further to the blue, indicating smaller particles in the pure ODPA synthesis. The presence of a higher concentration of larger particles and a higher MSC concentration indicates that the reactivity of the OPA-containing cadmium precursors is greater than that of the pure ODPA precursors; that is, the value of k_1 is larger with OPA in the cadmium precursor. This can be understood in terms of a larger diffusion coefficient of the precursor with the smaller ODA and is consistent with the diffusion-controlled model by Peng.[18] At later times, the exciton of the pure ODPA synthesis is further to the red than that in the OPA-containing synthesis, indicating the presence of larger particles in the pure ODPA synthesis. This is also consistent with the results reported by Wang *et al.*[6] Thus, in the later stages of the reaction, when only nanorods and monomers are present, the growth rate of the particles in the pure ODPA synthesis is greater than that in the OPA-containing synthesis. This indicates that the OPA-ligated particles are less reactive than ODPA-ligated ones. These results support the conclusion that both of the above mechanisms are operative in these syntheses.

Syntheses Using Technical-Grade TOPO and the Effect of Acids on Cadmium Precursor Reactivity. Many of the CdSe nanoparticle syntheses that have been reported have used various grades of unpurified TOPO. Figure 7 shows time-dependent spectra obtained in a synthesis reaction using technical-grade (90%) TOPO. The reaction is in every other way identical to that using purified TOPO, giving the spectra in Figure 1. There are several significant differences in the spectra. The most obvious difference is that the MSC peak in Figure 7 is far less intense and shorter lived than that in Figure 1. The rapid appearance and greater absorbance at 2−7 min of the exciton peak also makes clear that particle formation occurs much faster in unpurified TOPO. These observations indicate that the unpurified TOPO contains impurities that make both the precursors and the growing nanorods more reactive. Technical-grade TOPO is known to contain significant amounts of inorganic acids, specifically H_3PO_3 and H_3PO_4.[17] We suggest that it is primarily the presence of these acids that both increases the reactivity of the cadmium precursors and inhibits phosphonate binding onto the nanoparticle surfaces. To confirm this, we first determined the amount of these acids in this lot of TOPO. This was done by first extracting the acids from 2.00 g of ether phase TOPO into water, followed by a titration. The result indicates that this lot of TOPO contains 1.04 mol % of acid (total H_3PO_3 plus H_3PO_4). In the above synthesis, this corresponds to a cadmium to acid mol ratio of about 20:1. This amount of H_3PO_4 was added to purified TOPO, followed by removal of the excess water. A synthesis was then run using this TOPO, and the spectra are presented in Figure 7. The reactivity in the added acid synthesis is far greater than that in the purified TOPO and only slightly less than that in the unpurified TOPO. In both unpurified and added acid cases, the MSC peak is gone after about 4 min. Other syntheses show that doubling the acid to a 10:1 mol ratio almost completely eliminates the MSC peak from the early time spectra. We propose that the mechanism by which the acid increases the precursor reactivity is partial protonation of the phosphonates in the $Cd(phosphonate)_2$ precursors, as depicted in Scheme 3. The protonated phosphonate is less strongly bound to the cadmium, making the pre-

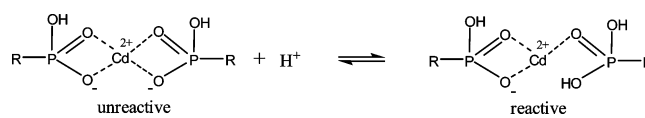

Scheme 3.

cursor less stable and more reactive. The same considerations apply to the phosphonate binding to cadmium atoms on the nanoparticle surfaces.

Technical-grade TOPO contains many different types of impurities: alkylphosphonic acids, alkylphosphinic acids, dialkyl phosphonic oxides, *etc.*[10,16,17] In this case, it is the presence of the inorganic acids that dominates the reactivity of the cadmium precursors. This can be understood in terms of the relative stabilities of different cadmium complexes.[17] The synthesis of CdSe nanorods requires the use of strongly binding phosphonate ligands; specifically, ODPA is used in the present syntheses. Except for octylphosphonic acid (OPA), all of the common impurities in TOPO are much less strongly binding than ODPA. As such, the presence of small amounts of these weaker binding ligands has little effect on the synthesis.

It is of interest to compare these results with those reported by Wang *et al.*[6] for a nominally identical reaction. Specifically, these authors present results for the "standard synthesis" described above, using reasonably pure (99%) TOPO and recrystallized ODPA. The nanorods have an absorbance maximum of 626 nm, following 8 min of reaction at 300 °C. Using identical conditions and concentrations, we find that an absorbance maximum of 626 nm occurs at about 10 min. Apparently, the precursors in used by Wang *et al.* are slightly more reactive than the ones used here. There are two possible reasons for this. First, it may be that the 99% TOPO has small but sufficient amounts of impurities (probably inorganic acids) to increase the reactivity of the cadmium precursor. Second, the selenium precursor is more reactive. The first possibility cannot be ruled out. However, other studies have used 99% TOPO in the synthesis of CdSe nanowires and found that it is of sufficient purity that it behaves like purified TOPO in most respects.[17] This observation argues against the difference being due to TOPO impurities. We conclude that the role of acid impurities in this slight reactivity increase must be viewed as unknown. The other possibility is that the increased reactivity is due to differences in the selenium precursor. In the results presented here, the TOP used to make the selenium precursor was distilled to remove any OPA, which is typically present in significant quantities. As noted above, the addition of 0.8 mmol of ODPA into the selenium precursor increases the reactivity of the reaction mixture. With this composition, the absorption spectrum has a maximum at 626 nm at 5 min after injection. The reactivity reported by Wang *et al.* is intermediate between ours made with pure TOP and with added phosphonic acid. This is consistent with the presence of phosphonic acids, specifically OPA, in unpurified TOP. These results underscore the need for purification of both TOP and TOPO to obtain reproducible results.

SUMMARY AND CONCLUSIONS

Several conclusions may be drawn from the results presented here.

(1) The overall CdSe nanorod synthesis reaction involves CdSe monomers and magic-sized clusters (MSCs) as intermediates. A reaction mechanism is proposed in which precursors react to form monomers and monomers react to form nanoparticles. In this mechanism, MSCs are in equilibrium with the monomers and therefore limit the monomer concentration to the saturation value. The observed MSC and particle growth kinetics can be accurately modeled by kinetic equations based on this mechanism. This model gives a monomer saturation value of about 8.1 mM in 300 °C TOPO.

(2) Changing the concentrations of TOP and ODPA in the reaction solution changes the rates of both the precursor to monomer and monomer to nanoparticle reactions. These rates increase or decrease together as the TOP and ODPA concentrations are varied, with the latter reaction rate being more sensitive to variations in concentration.

(3) The least reactive system studied contains cadmium in the form of $Cd(ODPA)_2$ and a TOP to Se mol ratio of about 6. There is a strong coupling between the effects of changing the ODPA and TOP concentrations in cadmium and selenium precursors, respectively. This is because the (highly oxidized) ODPA and (reduced) TOP components in the reaction mixture are coupled through an oxidative equilibrium.

(4) The reactivity of $Cd(phosphonate)_2$ precursors varies with the chain length of the alkyl phosphonates. Shorter alkyl chains result in higher reactivities. Shorter alkyl chains also result in the phosphonates binding more tightly to the radial surfaces of the growing nanorods. The combination of these factors results in higher aspect ratio particles.

(5) Addition of inorganic acids protonates the phosphonates, making this species more reactive. The presence of inorganic acids (impurities) is the primary reason that cadmium precursors made with technical-grade TOPO are much more reactive than those made with purified TOPO.

EXPERIMENTAL SECTION

Chemicals: Cadmium oxide (CdO, 99.5%), technical-grade trioctylphosphine oxide (TOPO, 90%), trioctylphosphine (TOP, 97%), tributylphosphine (TBP, 97%), potassium hydroxide aqueous solution (KOH, 1.0M), and toluene (99%) were received from Aldrich. Selenium (Se, 99%) and 1-octylphosphonic acid (OPA, 98%) were purchased from Alfa Aesar. Octadecylphosphonic acid (ODPA, 99%) was obtained from PCI synthesis. Phosphoric acid (H_3PO_4, 99%) and octane (≥99.0%) were obtained from Fluka. In some cases (as noted), TOPO was used as received. In all other cases, TOPO was twice recrystallized from acetonitrile, resulting in a pure, white crystalline powder. Further recrystallization had

no effect on the synthesis reactions. ODPA was recrystallized using toluene. TOP and TBP were vacuum distilled before use. In the case of TOP, the fraction between 202 and 205 °C was kept. Toluene was distilled from P_2O_5 prior to use. Millipore water (>18 MΩ · cm) was used in the titrations and in the phosphoric acid dilutions.

Titration of Inorganic Acid in TOPO: Two grams of 90% TOPO was dissolved in 30 mL of octane. An extraction of the inorganic acid in the solution was then done by mixing it with 30 mL of water. The water phase was removed and used in an acid−base titration with 2×10^{-2} M KOH to determine the concentration of the inorganic acid in TOPO. The second end point occurred at 5.4 mL of KOH, at pH 8.7, as determined using a pH meter.

Preparation of CdSe Nanorods: ***Cadmium Precursor.*** CdO (0.2054 g, 1.6 mmol), 2.930 g of TOPO, and predefined amounts of ODPA, OPA, and in some cases H_3PO_4 were loaded into a reaction flask (50 mL). The reaction mixture was the heated to 150 °C under vacuum and kept at that temperature for ≥0.5 h to remove traces of water. The flask was then flooded with N_2 gas and heated to 300−320 °C until all of the CdO reacted. This solution was kept at this temperature for 30 min and then cooled to room temperature under N_2 flow. After aging for at least 24 h, it was used without further purification.

Selenium Precursor. In a nitrogen glovebox, 0.063 g of Se and 0.19 g of TBP (0.253 g of solution having 25% Se by mass, 0.8 mmol of Se) were mixed with 1.447 g of TOP and 0.3 g of toluene to obtain the injection solution. In some case, 0.8 mmol of OPA or ODPA was added to this selenium precursor. In these cases, the precursor would solidify and would therefore have to be gently heated for injection into the cadmium precursor.

Cadmium Selenide CdSe Nanorods. The cadmium precursor was heated to 320 °C under N_2 flow. The selenium precursor loaded in a 10 mL syringe was then rapidly injected into the reaction flask. Following injection, the reaction temperature would drop to about 280 °C. The temperature was then brought back up to and kept at 300 °C for reaction. The color changes of the reaction mixture after selenium injection indicated the formation of CdSe nanorods. Taking the injection of selenium precursor as time zero, the aliquots were taken at predefined times for optical studies.

Characterization: Static fluorescence spectra were obtained using a Jobin-Yvon Fluorolog-3. The instrument consists of a xenon lamp/double monochromator excitation source and a CCD detector. UV−vis spectra were taken using a Cary 50 SCAN UV−vis spectrophotometer. TEM images were obtained on a JEOL 2010 transmission electron microscope.

Acknowledgment. This work was funded by the Division of Chemical Sciences, Geosciences, and Biosciences, Office of Basic Energy Sciences of the U.S. Department of Energy through Grant DE-FG02-04ER15502. The authors wish to acknowledge the use of the instrumentation and Mike Dunlap's assistance at the Imaging and Microscopy Facility at UC Merced. The authors also thank Prof. Matthew Meyer for his assistance with the ^{31}P NMR spectra.

REFERENCES AND NOTES

1. Peng, X.; Manna, L.; Yang, W.; Wickham, J.; Scher, E.; Kadavanich, A.; Alivisatos, A. P. Shape Control of CdSe Nanocrystals. *Nature* **2000**, *404*, 59–61.
2. Manna, L.; Scher, E. C.; Alivisatos, A. P. Synthesis of Soluble and Processable Rod-, Arrow-, Teardrop-, and Tetrapod-Shaped CdSe Nanocrystals. *J. Am. Chem. Soc.* **2000**, *122*, 12700–12706.
3. Qu, L.; Peng, X. Control of Photoluminescence Properties of CdSe Nanocrystals in Growth. *J. Am. Chem. Soc.* **2002**, *124*, 2049–2055.
4. Peng, Z. A.; Peng, X. Nearly Monodisperse and Shape-Controlled CdSe Nanocrystals *via* Alternative Routes: Nucleation and Growth. *J. Am. Chem. Soc.* **2002**, *124*, 3343–3353.
5. Peng, X. Mechanisms for the Shape-Control and Shape-Evolution of Colloidal Semiconductor Nanocrystals. *Adv. Mater.* **2003**, *15*, 459–463.
6. Wang, W.; Banerjee, S.; Jia, S.; Steigerwald, M. L.; Herman, I. P. Ligand Control of Growth, Morphology, and Capping Structure of Colloidal CdSe Nanorods. *Chem. Mater.* **2007**, *19*, 2573–2580.
7. Peng, Z. A.; Peng, X. Formation of High Quality CdTe, CdSe and CdS Nanocrystals Using CdO as a Precursor. *J. Am. Chem. Soc.* **2001**, *123*, 183–184.
8. Wu, D.; Kordesch, M. E.; Patten, P. G. V. A New Class of Capping Ligands for CdSe Nanocrystal Synthesis. *Chem. Mater.* **2005**, *17*, 6436–6441.
9. Mokari, T.; Banin, U. Synthesis and Properties of CdSe/ZnS Core/Shell Nanorods. *Chem. Mater.* **2003**, *15*, 3955–3960.
10. Liu, H.; Owen, J. S.; Alivisatos, A. P. Mechanistic Study of Precursor Evolution in Colloidal Group II−VI Semiconductor Nanocrystal Synthesis. *J. Am. Chem. Soc.* **2007**, *129*, 305–312.
11. Owen, J. S.; Park, J.; Trudeau, P.-E.; Alivisatos, A. P. Reaction Chemistry and Ligand Exchange at Cadmium Selenide Nanocrystal Surfaces. *J. Am. Chem. Soc.* **2008**, *130*, 12279–12281.
12. Kopping, J. T.; Patten, T. E. Identification of Acidic Phosphorus-Containing Ligands Involved in the Surface Chemistry of CdSe Nanoparticles Prepared in Tri-*n*-octylphosphine Oxide Solvents. *J. Am. Chem. Soc.* **2008**, *130*, 5689–5698.
13. Morris-Cohen, A. J.; Donakowski, M. D.; Knowles, K. E.; Weiss, E. A. The Effect of a Common Purification Procedure on the Chemical Composition of the Surfaces of CdSe Quantum Dots Synthesized with Trioctylphosphine Oxide. *J. Phys. Chem. C* **2010**, *114*, 897–906.
14. Embden, J. v.; Mulvaney, P. Nucleation and Growth of CdSe Nanocrystals in a Binary Ligand System. *Langmuir* **2005**, *21*, 10226–10233.
15. Talapin, D. V.; Nelson, J. H.; Shevchenko, E. V.; Aloni, S.; Sadtler, B.; Alivisatos, A. P. Seeded Growth of Highly Luminescent CdSe/CdS Nanoheterostructures with Rod and Tetrapod Morphologies. *Nano Lett.* **2007**, *7*, 2951–2959.
16. Wang, F.; Tang, R.; Buhro, W. E. The Trouble with TOPO: Identification of Adventitious Impurities Beneficial to the Growth of Cadmium Selenide Quantum Dots, Rods, and Wires. *Nano Lett.* **2008**, *8*, 3521–3524.
17. Wang, F.; Tang, R.; Kao, J. L.-F.; Dingman, S. D.; Buhro, W. E. Spectroscopic Identification of Tri-*n*-octylphosphine Oxide (TOPO) Impurities and Elucidation of Their Roles in Cadmium Selenide Quantum-Wire Growth. *J. Am. Chem. Soc.* **2009**, *131*, 4983–4994.
18. Peng, A.; Peng, X. Mechanisms of the Shape Evolution of CdSe Nanocrystals. *J. Am. Chem. Soc.* **2001**, *123*, 1389–1395.
19. Pradhan, N.; Xu, H.; Peng, X. Colloidal CdSe Quantum Wires by Oriented Attachment. *Nano Lett.* **2006**, *6*, 720–724.
20. Soloviev, V. N.; Eichhöfer, A.; Fenske, D.; Banin, U. Molecular Limit of a Bulk Semiconductor: Size Dependence of the "Band Gap" in CdSe Cluster Molecules. *J. Am. Chem. Soc.* **2000**, *122*, 2673–2674.
21. Soloviev, V. N.; Eichhöfer, A.; Fenske, D.; Banin, U. Size-Dependent Optical Spectroscopy of a Homologous Series of CdSe Cluster Molecules. *J. Am. Chem. Soc.* **2001**, *123*, 2354–2364.
22. Ouyang, J.; Zaman, M. B.; Yan, F. J.; Johnston, D.; Li, G.; Wu, X.; Leek, D.; Ratcliffe, C. I.; Ripmeester, J. A.; Yu, K. Multiple Families of Magic-Sized CdSe Nanocrystals with Strong Bandgap Photoluminescence *via* Noninjection One-Pot Syntheses. *J. Phys. Chem. C* **2008**, *112*, 13805–13811.
23. Chen, H. S.; Kumar, R. V. Discontinuous Growth of Colloidal CdSe Nanocrystals in the Magic Structure. *J. Phys. Chem. C* **2009**, *113*, 31–36.
24. Kasuya, A.; Sivamohan, R.; Barnakov, Y. A.; Dmitruk, I. M.; Nirasawa, T.; Romanyuk, V. R.; Kumar, V.; Mamykin, S. V.; Tohji, K.; Jeyadevan, B.; Shinoda, K.; Kudo, T.; Terasaki, O.; Liu, Z.; Belosludov, R. V.; Sundararajan, V.; Kawazoe, Y. Ultra-stable Nanoparticles of CdSe Revealed from Mass Spectrometry. *Nat. Mater.* **2004**, *3*, 99–102.

25. Kudera, S.; Zanella, M.; Giannini, C.; Rizzo, A.; Li, Y.; Gigli, G.; Cingolani, R.; Ciccarella, G.; Spahl, W.; Parak, W. J.; Manna, L. Sequential Growth of Magic-Size CdSe Nanocrystals. *Adv. Mater.* **2007**, *19*, 548–552.
26. Herron, N.; Calabrese, J. C.; Farneth, W. E.; Wang, Y. Crystal Structure and Optical Properties of $Cd_{32}S_{14}(SC_6H_5)_{36}$. DMF_4, a Cluster with a 15 Angstrom CdS Core. *Science* **1993**, *259*, 1426–1428.
27. Vossmeyer, T.; Reck, G.; Katsikas, L.; Haupt, E. T. K.; Schulz, B.; Weller, H. A "Double-Diamond Superlattice" Built Up of $Cd_{17}S_4(SCH_2CH_2OH)_{26}$ Clusters. *Science* **1995**, *267*, 1476–1479.
28. Yu, Q.; Liu, C.-Y. Study of Magic-Size-Cluster Mediated Formation of CdS Nanocrystals: Properties of the Magic-Size Clusters and Mechanism Implication. *J. Phys. Chem. C* **2009**, *113*, 12766–12771.
29. Li, M.; Ouyang, J.; Ratcliffe, C. I.; Pietri, L.; Wu, X.; Leek, D. M.; Moudrakovski, I.; Lin, Q.; Yang, B.; Yu, K. CdS Magic-Sized Nanocrystals Exhibiting Bright Band Gap Photoemission *via* Thermodynamically Driven Formation. *ACS Nano* **2009**, *3*, 3832–3838.
30. Dagtepe, P.; Chikan, V.; Jasinski, J.; Leppert, V. J. Quantized Growth of CdTe Quantum Dots: Observation of Magic-Sized CdTe Quantum Dots. *J. Phys. Chem. C* **2007**, *111*, 14977–14983.
31. Wang, R.; Ouyang, J.; Nikolaus, S.; Brestaz, L.; Zaman, M. B.; Wu, X.; Leek, D.; Ratcliffe, C. I.; Yu, K. Single-Sized Colloidal CdTe Nanocrystals with Strong Bandgap Photoluminescence. *Chem. Commun.* **2009**, 962–964.
32. Jiang, Z.-J.; Leppert, V.; Kelley, D. F. Static and Dynamic Emission Quenching in Core/Shell Nanorod Quantum Dots with Hole Acceptors. *J. Phys. Chem. C* **2009**, *113*, 19161–19171.
33. Tebby, J. C. *Handbook of Phosphorus-31 Nuclear Magnetic Resonance Data*; CRC Press: Boca Raton, FL, 1991.
34. Kim, J. I.; Lee, J.-K. Sub-kilogram-Scale One-Pot Synthesis of Highly Luminescent and Monodisperse Core/Shell Quantum Dots by the Successive Injection of Precursors. *Adv. Funct. Mater.* **2006**, *16*, 2077–2082.